Erratum

The correlation between locomotor performance and hindlimb kinematics during burst locomotion in the Florida scrub lizard, *Sceloporus woodi*

Eric McElroy, Kristen L. Archambeau and Lance D. McBrayer

10.1242/jeb.096776

There was an error published in *J. Exp. Biol.* **215**, 442-453.

In Table 2, the heading for columns 7 and 8 should have read ‘Combined’ rather than ‘Stride 3’. The correct version of the table is given below.

Table 2. Results of the hierarchical partitioning analysis

	Stride 1				Stride 3		Combined					
	Final speed		Peak mass-specific power		Final speed		Final speed		Total acceleration		Peak acceleration	
	I	*J*	*I*	*J*	*I*	*J*	*I*	*J*	*I*	*J*	*I*	*J*
Min. hip Θ	–	–	0.12	0.11	0.06	0.22	–	–	–	–	–	–
Min. knee Θ	–	–	–	–	0.15	0.28	–	–	0.11	0.17	0.10	0.17
Min. ankle Θ	0.06	–0.06	–	–	0.10	0.30	0.10	–0.05	–	–	–	–
Min. MTP Θ	0.15	0.20	–	–	0.05	0.17	0.10	0.09	–	–	–	–
Min. rotation Θ	–	–	–	–	–	–	–	–	0.14	0.22	0.15	0.17
Total Θ swept hip	–	–	–	–	0.09	0.16	–	–	–	–	–	–
Total Θ swept knee	–	–	–	–	–	–	–	–	0.08	0.17	0.07	0.20
Total Θ swept ankle	0.10	–0.04	–	–	–	–	0.04	–0.03	0.11	0.18	0.08	0.18
Total Θ swept MTP	0.14	0.28	–	–	0.08	0.20	0.07	0.11	–	–	–	–
Total Θ swept rotation	–	–	0.14	0.16	–	–	–	–	0.07	0.15	–	–
Θ V_{max} hip	–	–	–	–	–	–	–	–	0.10	0.02	–	–
Θ V_{max} knee	–	–	–	–	–	–	–	–	–	–	0.07	0.15
Θ V_{max} ankle	–	–	–	–	0.16	0.04	–	–	–	–	–	–
Θ V_{max} MTP	0.10	0.24	0.13	0.09	0.04	0.18	–	–	–	–	–	–
Θ V_{max} rotation	0.13	0.17	–	–	0.17	0.36	0.15	0.10	–	–	–	–

Only variables with a significant simple Pearson correlation, or 0.75 posterior probability in Bayesian model averaging, were included in the partitioning analysis. *I* is the variance explained by a predictor variable that is independent of the variance explained by other predictors (i.e. not influenced by collinearity) and is always a positive number or zero. *J* is the variance explained by collinearity between predictors. A positive *J* suggests that collinearity has inflated the simple correlation between the predictor and response, whereas a negative *J* suggests that collinearity has suppressed the simple correlation. The square root of the sum of *I* and *J* for each variable is the absolute value of its simple Pearson correlation.

MTP, metatarsophalangeal; Θ, angle; Θ V_{max}, maximum instantaneous angular velocity.

We apologise to authors and readers for any inconvenience this error may have caused.

The Journal of Experimental Biology 215, 442-453

doi:10.1242/jeb.058867

RESEARCH ARTICLE

The correlation between locomotor performance and hindlimb kinematics during burst locomotion in the Florida scrub lizard, *Sceloporus woodi*

Eric J. McElroy[1,*], Kristen L. Archambeau[1] and Lance D. McBrayer[2]

[1]Department of Biology, College of Charleston, Charleston, SC 29401, USA and [2]Department of Biology, Georgia Southern University, Statesboro, GA 30460, USA

* Author for correspondence (mcelroye@cofc.edu)

Accepted 26 September 2011

SUMMARY

Burst locomotion is thought to be closely linked to an organism's ability to survive and reproduce. During the burst, animals start from a standstill and then rapidly accelerate to near-maximum running speeds. Many previous studies have described the functional predictors of maximum running speed; however, only recently has work emerged that describes the morphological, functional and biomechanical underpinnings of acceleration capacity. Herein we present data on the three-dimensional hindlimb kinematics during burst locomotion, and the relationship between burst locomotor kinematics and locomotor performance in a small terrestrial lizard (*Sceloporus woodi*). We focus only on stance phase joint angular kinematics. *Sceloporus woodi* exhibited considerable variation in hindlimb kinematics and performance across the first three strides of burst locomotion. Stride 1 was defined by larger joint angular excursions at the knee and ankle; by stride 3, the knee and ankle showed smaller joint angular excursions. The hip swept through similar arcs across all strides, with most of the motion caused by femoral retraction and rotation. Metatarsophalangeal (MTP) kinematics exhibited smaller maximum angles in stride 1 compared with strides 2 and 3. The significant correlations between angular kinematics and locomotor performance were different across the first three strides. For stride 1, MTP kinematics predicted final maximum running speed; this correlation is likely explained by a correlation between stride 1 MTP kinematics and stride 2 acceleration performance. For stride 3, several aspects of joint kinematics at each joint predicted maximum running speed. Overall, *S. woodi* exhibits markedly different kinematics, performance and kinematics–performance correlations across the first three strides. This finding suggests that future studies of burst locomotion and acceleration performance should perform analyses on a stride-by-stride basis and avoid combining data from different strides across the burst locomotor event. Finally, the kinematics–performance correlations observed in *S. woodi* were quite different from those described for other species, suggesting that there is not a single kinematic pattern that is optimal for high burst performance.

Supplementary material available online at http://jeb.biologists.org/cgi/content/full/215/3/442/DC1

Key words: lizard, locomotion, performance, kinematics, acceleration.

INTRODUCTION

Locomotor performance (i.e. sprint speed, endurance, acceleration, etc.) is a key intermediate between organismal morphology and fitness and ecology (e.g. Arnold, 1983; Garland and Losos, 1994; Irschick and Garland, 2001; LeGalliard et al., 2004; Husak et al., 2006; Calsbeek and Irschick, 2007). However, variation in morphology may not directly translate to variation in performance, as the link between morphology and performance can be impacted by biomechanics and physiology (Reilly and Wainwright, 1994). Thus, a detailed understanding of function is required to quantify the nature of evolutionary transitions in morphology–performance–fitness relationships.

Most previous studies of locomotor performance have focused on steady-state locomotion in which the movement is uniform, such as when an animal is moving at a constant, maximal speed (Garland and Losos, 1994; Irschick and Garland, 2001; McElroy et al., 2008). However, in nature, animals often do not move at steady speed (see Kramer and McLaughlin, 2001), and thus selection may not directly act on locomotor performance at a steady speed. Correlations between steady-speed performance in the laboratory and fitness are potentially spurious, and more ecologically relevant studies of locomotor behavior are warranted. Studying non-steady-state locomotion may provide a more realistic connection between locomotor performance and organismal fitness. In particular, lizards often exhibit bursts of movement, with bouts of acceleration and deceleration (Vanhooydonck et al., 2006a; Vanhooydonck et al., 2006b) being used in a variety of behavioral contexts such as foraging, social interactions and fleeing from predators (Irschick and Losos, 1998; McElroy et al., 2007).

Recent years have seen a tremendous growth in the number of studies examining non-steady-state locomotion, particularly acceleration performance. These studies demonstrate the relevance of underlying morphological, physiological and functional parameters to acceleration performance (Delecluse, 1997; Vanhooydonck et al., 2006a; Vanhooydonck et al., 2006b; Williams et al., 2009). For example, both limb length and muscle mass are positively correlated with high sprint speeds and acceleration capacity (Losos, 1990; Garland and Losos, 1994; Vanhooydonck et al., 2006a; Higham et al., 2011). In addition, hip, knee and ankle joints and their associated musculature have been repeatedly shown to predict acceleration in variety of quadrupedal vertebrates, although

the exact joints and muscles involved appear to vary across species (Williams et al., 2009; Higham et al., 2011). Thus, a general understanding of acceleration performance and mechanics seems to be emerging, but many details are still lacking.

Two central issues are crucial for understanding the relationship between kinematics and performance. First, acceleration performance is typically maximal when an animal bursts from a standstill to near-maximal speeds (e.g. Vanhooydonck et al., 2006b; McElroy and McBrayer, 2010; Higham et al., 2011). As burst locomotion progresses, locomotor performance changes from maximizing acceleration to maximizing speed, and thus kinematics are likely to change. Second, if locomotor kinematics and performance are changing from stride-to-stride during burst locomotion, then the relationship between kinematics and performance is also likely to change from stride-to-stride. These two important aspects have yet to be examined, despite a suite of recent studies on acceleration performance where data from different strides were combined to compute a single regression or correlation (e.g. McGowan et al., 2005; Williams et al., 2009). Combining strides could have a profound impact on the interpretation of the data and the development of any general principles underlying non-steady-state locomotor performance.

The goal of this study was to examine the relationship between limb kinematics and whole-animal performance during burst locomotion. We asked three questions: (1) do joint angular kinematics change across strides as an animal accelerates from a standstill; (2) do per-stride joint angular kinematics predict per-stride whole-animal performance; and (3) what effect does analyzing locomotor data on a per-stride *vs* combined strides basis have on the interpretation of the kinematic factors underlying locomotor performance? To address these questions, we collected kinematic and performance data from a small terrestrial lizard (*Sceloporus woodi*) as it burst from standstill through the first three strides of locomotion. We examined kinematic variables associated with angular motion of the hindlimb joints [hip, knee, ankle and metatarsophalangeal (MTP)]. In particular, we measured key aspects of motion for each joint: the minimum and maximum angles, total angular excursion and the peak angular velocity. At the hip, three-dimensional (3-D) motion was decomposed into rotation, abduction–adduction and retraction–protraction. These angular variables were chosen because the angles through which these joints sweep can be conceptually linked to relevant aspects of muscle morphology and physiology (e.g. the angle the knee sweeps through during extension can be linked to mm. ambiens function) and may guide future functional studies regarding which muscles drive locomotor performance. Previous studies have suggested that the knee extensors and hip retractors are the most important muscle groups involved in speed and acceleration in lizards (Reilly and Delancey, 1997; Nelson and Jayne, 2001; Vanhooydonck et al., 2006a). However, several other studies (Miles, 1994; Bauwens et al., 1995; Irschick and Jayne, 1999; Vanhooydonck et al., 2006a; Miles et al., 2007) have suggested that the lengths of the distal limb bones (tibia, metarsus and toes) are important predictors of maximum sprint speed. Thus, we expected that angular kinematics at the hip and knee joints would be better predictors of acceleration and mass-specific power than those at the ankle and MTP, whereas angular kinematics at the ankle and MTP would be better predictors of final speed than those at the hip and knee.

MATERIALS AND METHODS

Animals

Ten adult male *Sceloporus woodi* (Stejneger 1918) were captured in the Ocala National Forest in central Florida during April and June 2009. The lizards were individually housed in aquaria containing loose, sandy substrate. They were fed vitamin-dusted crickets three times per week and misted with water daily. Only healthy individuals were used in the experiments. The animals were warmed to 35°C for 1 h before each trial and between trials performed on the same day. Lizards were rested for at least 30 min between trials held on the same day and were ran on at least three separate days with 2 days rest between experimental days.

Before any trials were conducted, lizards were weighed (0.1 g) and then a small spot of non-toxic white correction fluid was painted on the six markers indicated in Fig. 1. An additional dot was painted at the base of the lizards' head. These markers were later used as digitization landmarks in the high-speed video records to obtain the kinematic data. These landmarks enable the straightforward calculation of the kinematic variables that are likely to change during burst locomotion (i.e. high accelerative steps initially transitioning to steps that maintain high speed) (McElroy and McBrayer, 2010). The hip marker was typically placed ~1 mm from the location of the acetabulum; very minor variation in the placement of the acetabulum marker introduced error into our kinematic computations that was always <5%, and more typically <3%. Because we could not precisely adjust the position of the hip marker for each lizard (we lacked radiographs) (see Jayne and Irschick, 1999), we chose to proceed with all analyses based on the marked position of the hip on the animal. All methods followed approved IACUC protocols (Georgia Southern: I08009; College of Charleston: 2009-009).

Trials

The lizards ran down a horizontal racetrack towards a dark hide box. The racetrack was 3 m long and 0.35 m wide, with wooden sidewalls 0.4 m tall. Cork bark covered the track's surface providing traction; we rarely observed foot slippage in the video. A Casio EXILIM EX-F1 camera (512×384 pixel resolution, Casio America, Dover, NJ, USA) was suspended over the track in order to collect a vertical view of the lizard over the first 0.4 m of the track. A second Casio EXILIM EX-F1 camera was placed on a tripod next to the track in order to obtain a lateral view of the lizard over the first 0.4 m of the track. All video was recorded at 300 frames s^{-1}.

Lizards were placed at the beginning of the track so that their entire bodies could be seen in the camera. The lizards were initially motionless. In order to observe a rapid burst of motion from rest, the lizards were startled by hand clapping or a light tail pinch. Continuous clapping encouraged the lizard to run all the way down the track and out of the cameras' view. Each individual ran down the track five to 10 times with at least 30 min of rest between each run and with each individual being run on three or more separate days. Trials were excluded if lizards ran at an angle, moved slowly

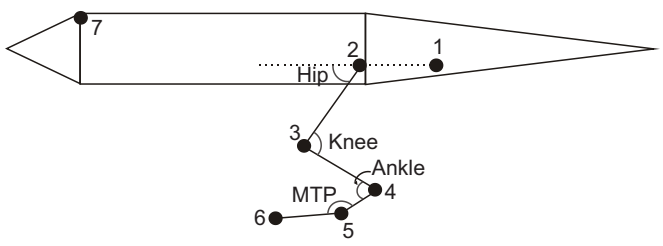

Fig. 1. Lateral-view schematic of kinematic markers (1–7) and hindlimb joint angles. MTP, metatarsophalangeal. The angles depicted are three-dimensional. Dotted line represents a horizontal line connecting markers 1 and 2, which was used as a reference for computing angles of femoral protraction–retraction and abduction–adduction.

or stopped. This selection process resulted in a total of 20 trials from 10 individuals being retained for analysis (i.e. a single trial from six individuals, two trials from two individuals and three trials from two individuals).

Video analysis

Raw video was imported and manually trimmed using Adobe Premiere Elements software (Adobe Systems, San Jose, CA, USA). The vertical and horizontal videos were synchronized *via* a light pulse that was visible in both cameras' field of view. Individual trials were trimmed to 10 frames before the lizard's initial movement until the lizard was completely out of the camera's view, yielding video of the first 0.4 m of locomotion from a standstill.

The video from the dorsal view was used to estimate the lizard's position for each frame. Using DIDGE software (Cullum, 1999), we manually digitized the white marker at the base of the back of the head to obtain the lizard's position. The point on the head was chosen because the head stayed relatively straight, rather than tracking left to right with medio-lateral bending as was observed at positions closer to the center of mass (e.g. the hips). Additionally, the front of the body rarely lifted from the substrate (only six of 60 strides were bipedal, and these strides occurred without noticeable head lifting); thus, we are confident that tracking at the head marker is a useful technique for estimating whole-animal performance in this species [as opposed to other species that may show considerable lifting due to bipedalism (e.g. Clemente et al., 2008)]. Next, we used the program GCVSPL (Woltring, 1986) to fit a quintic spline to the position data and calculate the first and second derivatives of the spline coefficients fitted to the position data (see also McElroy and McBrayer, 2010). This procedure yielded the instantaneous velocity and acceleration for each frame of the video. We also computed instantaneous external mechanical power by multiplying instantaneous velocity by acceleration by the lizard's body mass. From these data we calculated four performance variables: final speed (i.e. the maximum instantaneous speed obtained, always during stride 3); per-stride total acceleration [i.e. integral of the acceleration–time curve over stance phase per stride (McElroy and McBrayer, 2010)], per-stride peak acceleration (i.e. maximum value of the acceleration–time curve for each stride), and per-stride body mass-specific instantaneous peak whole-animal external mechanical power (i.e. peak of the power–time curve divided by body mass per stride).

Three-dimensional analysis was performed using DLTdv3 software (Hedrick, 2008) in MATLAB (MathWorks, Natick, MA, USA). First, we constructed a 3-D cube using Lego blocks and used white correction fluid to mark 13 points on the cube. The first frame of each video sequence from the horizontal and vertical views of the cube was used to calibrate the field of view using DLTcal3 (Hedrick, 2008) in MATLAB. Next, we uploaded vertical and horizontal videos for each trial and digitized all markers in each frame from foot touchdown to foot lift-off for each stride (i.e. stance phase). We focused on 3-D limb kinematics during stance phase only, as this is the only part of the locomotor cycle when force, and thus acceleration, can be generated (Curtin et al., 2005; McGowan et al., 2005; Williams et al., 2009; Higham et al., 2011). The end result of the 3-D kinematic analysis was the instantaneous *xyz* coordinate data for each kinematic marker during stance phases across several strides.

During stance phase, we calculated the instantaneous 3-D angles at the hip, knee, ankle and MTP joints. We transformed *xyz* coordinate data into 3-D joint angles using the following procedure. The hip position was fixed in each frame by subtracting the *x*, *y* and *z* coordinates of the hip marker (marker 2) from each point (markers 1–6) in each frame. The 3-D angle of the hip joint was found by taking the arccosine of the dot product of two vectors whose bases were at the hip (marker 2) and whose tips were at the knee (marker 3) and caudofemoralis origin (marker 1). To perform this matrix operation we used the following simple algebraic formula in Microsoft Excel:

$$\text{Hip}\theta = \text{arccosine}\left(\frac{(x_1x_2 + y_1y_2 + z_1z_2)}{\sqrt{x_1^2 + y_1^2 + z_1^2}\sqrt{x_2^2 + y_2^2 + z_2^2}}\right). \quad (1)$$

This process was repeated to calculate the 3-D angle at the knee (markers 2 and 4), ankle (markers 3 and 5) and MTP (markers 4 and 6). From this we could determine the minimum angle, maximum angle and total angle swept of the hip, knee, ankle and MTP for the first several strides of burst locomotion. Additionally, a quintic spline was fitted to the data and the first derivative, corresponding to the instantaneous angular velocity, was calculated. From this angular velocity data, we estimated maximum instantaneous angular velocity for each stride at each joint. Finally, the hip joint is a ball-and-socket joint; therefore, we also computed joint angular motion in the horizontal (protraction–retraction), vertical (abduction–adduction) planes as well as the femoral rotation. Femoral rotation was defined as the angle between two planes: (1) a vertical plane through the femur and (2) the plane containing the hip, knee and ankle markers (i.e. the plane formed by the thigh and shank). To determine the angle between these planes, we computed the dot product of their normal vectors. Normal vectors were computed by taking the cross product of two vectors contained within the plane.

We report angles such that increasing values would correlate with concentric contraction of the musculature responsible for producing joint motion hypothesized to be correlated with burst locomotion [i.e. femoral retraction, knee, ankle and MTP extension (Vanhooydonck et al., 2006a)]. For example, knee angles were relatively small when the knee was flexed near touchdown and then increased throughout stance as the knee extensor musculature and/or tendons were shortening. To force the hip angles to be increasing throughout stance phase (as the caudofemoralis muscle presumably concentrically contracts), this required calculating the dot product as mentioned above (markers 1, 2 and 3), and then taking the resulting angles and subtract them from 180 deg. Fig. 1 provides a summary schematic of the kinematic markers and joint angles. Because of the positioning of the lateral view camera, all data were collected for footfalls from the animal's left hindlimb only. We note that researchers with two camera systems are often constrained to collect data in this way, making it impossible to quantify kinematics for every step for every trial. This resulted in steps 1, 2 and 4 being collected from some individuals because steps 3 and 5 were obscured in lateral view, and steps 1, 3 and 5 being collected from other individuals because steps 2 and 4 were obscured by the body in lateral view. To help ameliorate these differences and proceed with statistical analyses, we coded all data by stride number (stride 1=step 1, stride 2=step 2 or 3, stride 3=step 4 or 5) for further analysis. We provide additional analyses (see below) to explore how this choice of grouping impacts the results.

Statistical analysis

We used JMP7 and SAS 9.2 (SAS Institute, Cary, NC, USA) and R v.2.10.1 (R Development Core Team, 2009) for all analyses. All variables were checked for normality and transformed, if necessary, prior to analysis.

Limb kinematics and whole-animal performance were characterized across the first three strides of burst locomotion. We used three analyses to explore stride-to-stride variation in joint kinematics. First, we quantified several variables that are traditionally reported for joint kinematics and performance, including: maximum joint angle, minimum joint angle, joint angular excursion, peak joint angular velocity, final (whole-animal) speed, acceleration, peak acceleration and mass-specific power. Next, we computed a canonical discriminant function analysis (DFA) with joint angular variables as independent variables and stride number as the classification variable to assess how well joint kinematics discriminate strides. Joint angular variables were those listed in Table 1 except for maximum joint angles. Angular maxima could not be included in DFA (or in Bayesian model averaging or MANOVA, see below) as they are the exact difference between angular excursions and angular minima, which makes the maxima perfectly collinear in a model that included both the minima and the excursions; perfect collinearity results in a singular covariance matrix and makes multivariate matrix computations impossible. To probe how our choice of grouping steps into strides (e.g. stride 2=step 2 or 3) affected the interpretation of our results, we computed two additional DFAs using step number as the classification variable and joint kinematics or locomotor performance as the covariates. From these DFAs, we generated classification tables to explore how our stride- *vs* step-based grouping affects the percentage of misclassified steps. Finally, we ran separate univariate mixed-model ANOVAs (using PROC MIXED in SAS) for each kinematic/performance variable (response) with stride number as the fixed effect and individual identity as a random effect. Strides were assigned to *post hoc* groupings using Tukey's honestly significant difference (HSD) tests. Finally, to examine whether the six observed bipedal strides exhibited functional differences, we computed two DFAs with gait (bipedal *vs* quadrupedal) as a classification variable and joint kinematics or performance as covariates.

We used generalized linear mixed models (GLMMs) to statistically compare the mean shape of the kinematic profile across strides and through time for each stride at each joint (see also Nauwelaerts and Aerts, 2003). This type of analysis uses the entire kinematic profile within each stride, as opposed to just a few variables computed from each stride's profile as in the previous analysis. By analyzing the entire kinematic profile when comparing stride-to-stride kinematics, we have the potential to uncover subtle differences in joint kinematics. Additionally, GLMM allows us to include multiple random effects with a variety of covariance structures whose parameters can be varied across the fixed effect. Our data were doubly repeated-measures; they involved multiple measurements of joint angles over time within a stride and multiple strides measured per individual. Thus, our random effects in the GLMM were: (1) time by individual, with a radial smoothing spline as the covariance structure whose parameterization was varied for each stride; and (2) stride by individual, with a simple unstructured covariance structure. By declaring both of these random effects in the model, we were able to statistically account for their impact on the test of the fixed effects (i.e. stride number, time and their interaction). Prior to running the GLMM, we rescaled the time axis for each stride for each individual to range from 0 to 1. This was done to help ameliorate the effect of timing differences on the comparison of kinematic profile shapes. We used PROC GLIMMIX in SAS 9.2 to fit the GLMM.

A common practice in studies of locomotion is to collect multiple trials per individual, and this often results in unequal numbers of trials per individual. We collected a single trial from six individuals,

Table 1. Pearson correlations between kinematic and performance variables

	Stride 1				Stride 2				Stride 3				Combined strides			
	Final speed	Total acceleration	Peak acceleration	Power	Final speed	Total acceleration	Peak acceleration	Power	Final speed	Total acceleration	Peak acceleration	Power	Final speed	Total acceleration	Peak acceleration	Power
Min. hip Θ	–0.13	–0.28	–0.33	–0.48*	–0.01	0.08	0.20	0.20	0.53*	–0.20	0.00	0.14	0.04	0.31	0.31	0.05
Min. knee Θ	0.02	–0.02	–0.07	–0.20	0.29	0.09	0.20	0.32	0.66**	0.12	0.29	0.38	0.22	–0.52*	–0.52*	–0.24
Min. ankle Θ	0.04	–0.39	–0.34	–0.25	0.02	–0.07	–0.01	–0.01	0.63**	0.06	0.49*	0.60*	0.22	–0.39	–0.35	–0.21
Min. MTP Θ	–0.59**	0.28	0.01	–0.30	–0.29	0.23	0.02	–0.25	–0.47*	0.20	0.02	–0.05	–0.43*	–0.08	–0.20	–0.30
Min. rotation Θ	–0.22	–0.05	–0.16	–0.39	0.08	0.18	0.29	0.29	–0.40	0.12	–0.13	–0.22	–0.14	0.60*	0.57**	0.21
Total Θ swept hip	0.19	0.19	0.26	0.41	–0.00	–0.24	–0.28	–0.21	–0.49*	–0.01	–0.16	–0.28	–0.07	–0.07	–0.05	0.05
Total Θ swept knee	0.10	0.11	0.18	0.25	–0.18	0.32	0.20	–0.04	–0.41	–0.15	–0.10	–0.18	–0.09	0.50*	0.52*	0.32
Total Θ swept ankle	0.23	0.36	0.27	0.21	0.19	0.40	0.37	0.20	–0.19	–0.07	–0.26	–0.30	0.10	0.53*	0.51*	0.36
Total Θ swept MTP	0.65**	–0.30	0.03	0.37	0.10	–0.25	–0.15	0.02	0.54*	–0.07	0.02	0.08	0.43*	–0.09	0.04	0.21
Total Θ swept rotation	0.38	–0.01	0.29	0.55**	0.37	–0.28	–0.16	0.07	0.40	–0.11	–0.05	0.03	0.31	–0.47*	–0.38	0.02
Θ V_{max} hip	0.16	–0.20	0.11	0.29	–0.08	–0.31	–0.23	–0.13	–0.02	–0.26	0.04	–0.01	0.03	–0.34	–0.21	0.02
Θ V_{max} knee	0.18	–0.19	0.09	0.19	0.09	0.43*	0.44*	0.28	0.32	–0.26	0.15	0.20	0.15	0.37	0.47*	0.32
Θ V_{max} ankle	0.36	–0.19	0.13	0.17	0.23	0.37	0.39	0.26	0.44*	–0.09	0.06	0.12	0.26	0.28	0.37	0.30
Θ V_{max} MTP	0.59**	–0.15	0.28	0.47*	0.34	0.11	0.13	0.20	0.47*	–0.02	0.02	0.07	0.41	–0.17	–0.05	0.18
Θ V_{max} rotation	0.55**	–0.10	0.13	0.21	0.11	–0.10	–0.05	0.16	0.72***	–0.22	–0.05	0.08	0.51*	–0.12	0.01	0.16
Max. hip Θ	0.05	–0.13	–0.12	–0.13	–0.01	–0.16	–0.05	0.03	–0.19	–0.22	–0.24	–0.28	–0.03	0.30	0.32	0.12
Max. knee Θ	0.11	0.11	0.15	0.12	0.01	0.48*	0.42	0.21	0.26	–0.05	0.22	0.23	0.11	0.11	0.15	0.18
Max. ankle Θ	0.30	0.15	0.09	0.07	0.18	0.29	0.31	0.17	0.63**	0.02	0.39	0.51*	0.34	0.21	0.23	0.19
Max. MTP Θ	–0.10	0.05	0.08	0.02	–0.36	–0.06	–0.27	–0.44*	0.11	0.21	0.07	0.04	–0.10	–0.29	–0.31	–0.21
Max. rotation Θ	0.34	–0.09	0.27	0.40	0.47*	–0.14	0.10	0.35	–0.02	0.02	–0.23	–0.25	0.25	0.21	0.31	0.34

Significance was determined by *t*-test (*P<0.05; **P<0.01; ***P<0.001). For the combined stride analysis, the degrees of freedom of the significance test were adjusted to be same as the separate stride analysis, such that the significant correlations could be directly compared between matrices. Underlined values had a posterior probability of being included in a 'good' multiple regression mode of >0.75, as determined by Bayesian model averaging.
MTP, metatarsophalangeal; Θ, angle; Θ V_{max}, maximum instantaneous angular velocity.

two trials from two individuals and three trials from two individuals. This creates a statistical issue where complex linear models cannot be fit because of unbalanced data sets (e.g. three samples from some individuals and only two from different individuals). We addressed this issue by using a nesting approach in which we declared the random effect as sample number nested within individual in both the univariate mixed models and the GLMMs. This allowed us to include all of the data to estimate the parameters of the mixed model whilst appropriately specifying denominator degrees of freedom in the hypothesis test.

In a second set of analyses, we estimated the importance of limb kinematics as predictors of whole-animal performance. Mass was significantly correlated with several kinematic variables, thus we computed the residuals of regressions of each kinematic variable on mass for each stride and used those for subsequent analyses. Performance variables were not correlated with mass (maximum speed: $r<0.001$, $P=0.88$; peak acceleration: $r<0.001$, $P=0.86$, total acceleration: $r<0.001$, $P=0.92$; mass-specific power: $r<0.001$, $P=0.88$). First, we computed simple Pearson univariate correlations between each kinematic and performance variable for each stride and then tested each correlation with a *t*-test. To account for the inherent multivariate nature of the kinematic data, we used a Bayesian model averaging method to estimate the importance of each kinematic predictor for each performance for each stride within a multiple regression framework (Ellison, 1996). Choosing the 'best' multiple regression model has many well-known issues; Bayesian model averaging accounts for the uncertainty in choosing the single best model by generating a posterior sample of 'good' models using a leaps-and-bound algorithm. From this sample of models, the method computes the posterior probability that a predictor variable has a non-zero coefficient. Given the nature of kinematic data, our predictor variables (kinematics) were often inter-correlated, which can create issues when attempting to interpret simple Pearson correlations (Chevan and Sutherland, 1991) and when attempting to compute multiple regression coefficients (Quinn and Keough, 2003). These inter-correlations make it difficult for one to know whether each simple correlation and/or regression coefficient is due to the predictor of interest independently, or due to collinearity between the predictor and other predictors (Quinn and Keough, 2003). Hierarchical partitioning is a statistical tool that can help disentangle independent correlation *vs* correlation that is due to collinearity (Chevan and Sutherland, 1991; Mac Nally, 2000; Mac Nally, 2002). This analysis works by computing all possible regression models and then comparing subsets of models with and without the predictor variable of interest. The increase in R^2 because of the inclusion of the predictor can be averaged across all comparisons to compute the independent contribution of that variable to the variance explained. The analysis also determines the joint contribution of other variables to the variance explained by the predictor of interests (i.e. the variance explained by collinearity with other predictors). Positive joint contribution values show that collinearity has inflated with correlation whereas negative joint values indicate suppression of the correlation. We computed hierarchical partitions for each performance variable for each stride, using 'important' predictors that were defined as having: (1) significant simple correlation coefficients or (2) a posterior probability of a non-zero coefficient greater than 0.75 (Kass et al., 1995). Only a subset of predictors was used in the partition because: (1) including all predictors (i.e. 14) is beyond the current computational abilities of 'hier.part' package, and (2) predictors that were not deemed 'important' by Pearson correlation or Bayesian model averaging were unlikely to reveal any additional information *via* partitioning their variance. We used the R packages 'hier.part' (Walsh and Mac Nally, 2008) for hierarchical partitioning and 'BMA' for Bayesian model averaging (Raftery et al., 2005).

Preliminary video review showed that stride 1 (i.e. the first movement from standstill) consisted of either a single leg push-off or a simultaneous double leg push-off. We tested for differences related to this behavioral variation by running two separate MANOVAs, one with the kinematic variables for stride 1 as responses, and one with performance variables for stride 1 as responses. In both MANOVAs, burst behavior (i.e. single- *vs* double-leg push-off) was the main effect.

Separate *vs* combined strides analysis

First, we computed the Pearson correlation between kinematics and performance after combining data across all strides. Next, we computed the Euclidean distance matrix from each of the four correlation matrices (stride 1, stride 2, stride 3 and combined strides). We then compared the distance matrix for the combined strides data with each of the distance matrices for the separate strides data using Mantel tests.

RESULTS

Comparison of joint angular changes across strides during burst locomotion

Lizards ranged from 2.0 to 4.4 g (mean: 2.9 g). Trials were mostly quadrupedal; only six of 60 strides were bipedal. Bipedal and quadrupedal strides did not differ in performance (Wilks' $\lambda=0.893$, $F_{4,55}=1.65$, $P=0.17$) or kinematics (Wilks' $\lambda=0.641$, $F_{15,44}=1.64$, $P=0.10$). Several of the kinematic variables showed significant changes across the first three strides of burst locomotion (Figs 2–6).

DFA found that stride number was significantly classified according to joint kinematics (Wilks' $\lambda=0.148$, $F_{24,92}=6.13$, $P<0.001$). DFA misclassified 10% of the observations (six of 60). All six misclassified strides were misclassified as an adjacent stride (e.g. stride 1 as stride 2). DF1 accounted for 84% of the variance and clearly separated the data into three groups (Fig. 2).

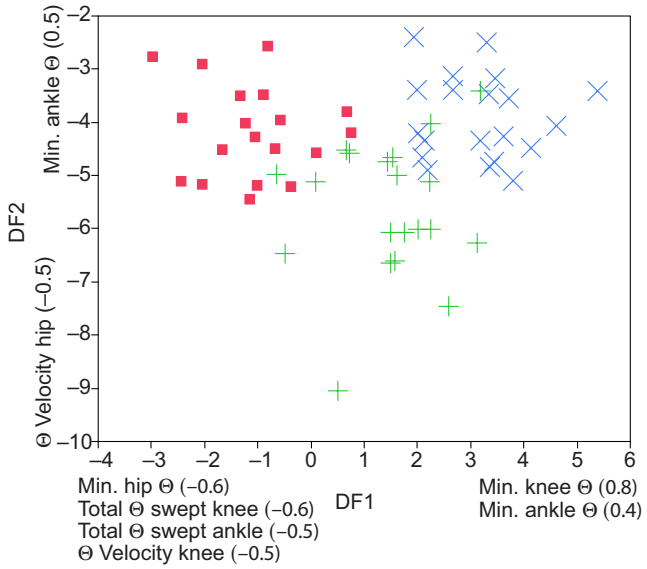

Fig. 2. Results of the discriminant function analysis with stride as the classification variable. The best discriminating variables are labeled at the ends of each axis with their loading in parentheses. All other variables had loadings between –0.3 and 0.3. Stride 1, red squares; stride 2, green pluses; stride 3, blue crosses. Θ, angle; Θ Velocity, V_{max}.

Standardized coefficients between the original variables for DF1 largely agreed with the results of the univariate mixed models: minimum hip and knee angles, ankle and knee angular excursion, and maximum knee speeds are the best discriminators of stride-to-stride kinematics. DF2 accounted for 16% of the variation and appeared to separate stride 2 from strides 1 and 3. Minimum ankle angle and maximum hip speed were the best discriminators for DF2.

The GLMMs and univariate mixed models showed the several differences in kinematics between strides (Figs 3–6).

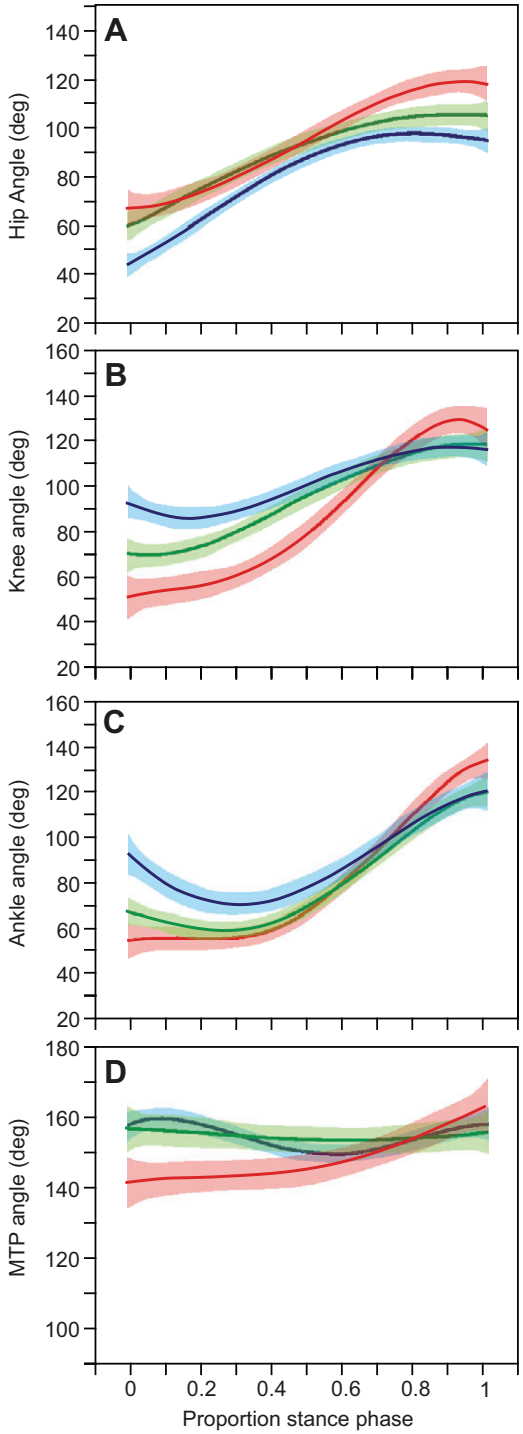

Fig. 3. Three-dimensional angular kinematics for the (A) hip, (B) knee, (C) ankle and (D) metatarso-phalangeal (MTP) joints. Data are normalized to the proportion of stance phase and are presented as raw data with the fitted smoothing spline (smoothed line) and its 95% confidence intervals (semi-transparent envelope around smoothed line). Colors: red, stride 1; green, stride 2; blue, stride 3.

Hip

The overall shape of the kinematic profiles was significantly different across strides (stride×spline interaction: $F_{30,269}$=2.45,

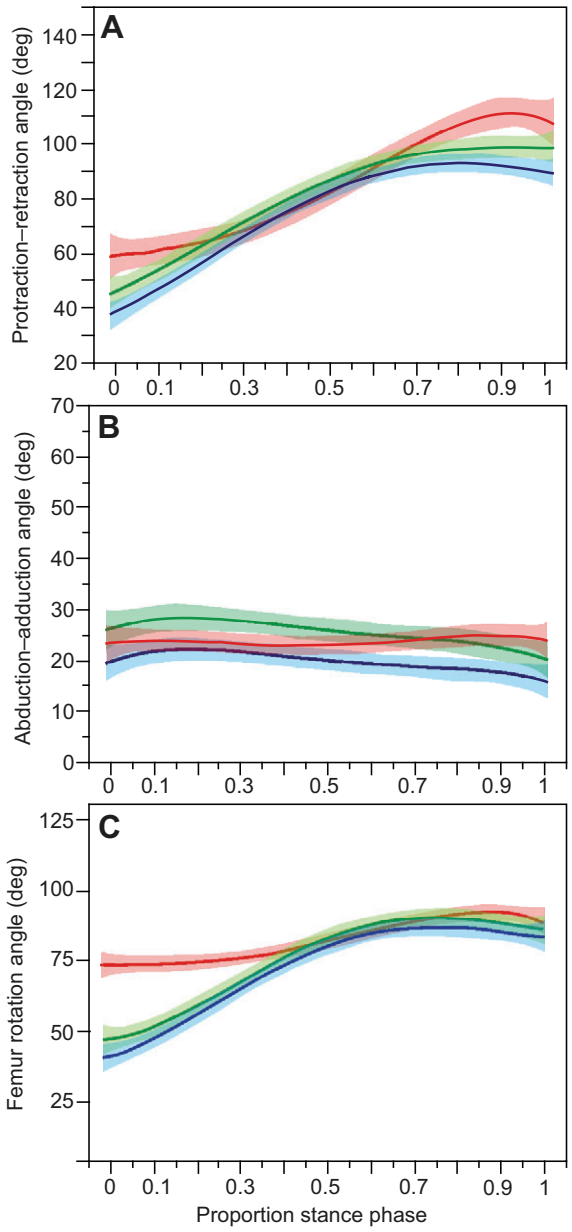

Fig. 4. Angle of femur (A) protraction–retraction, (B) abduction–adduction and (C) rotation. For protraction–retraction, an angle of 0 deg indicates that the femur is parallel (with the knee pointed rostrally) to the plane running vertically through the line defined between markers 1 and 2 (shown in Fig. 1). For abduction–adduction, an angle of 0 deg indicates that the femur is parallel to the horizontal plane going through the line created by markers 1 and 2. For femur rotation, an angle of 0 deg indicates that the plane formed by the thigh and shank is perpendicular to the ground whereas an angle of 90 deg indicates that the plane is parallel to the ground. Colors: red, stride 1; green, stride 2; blue, stride 3.

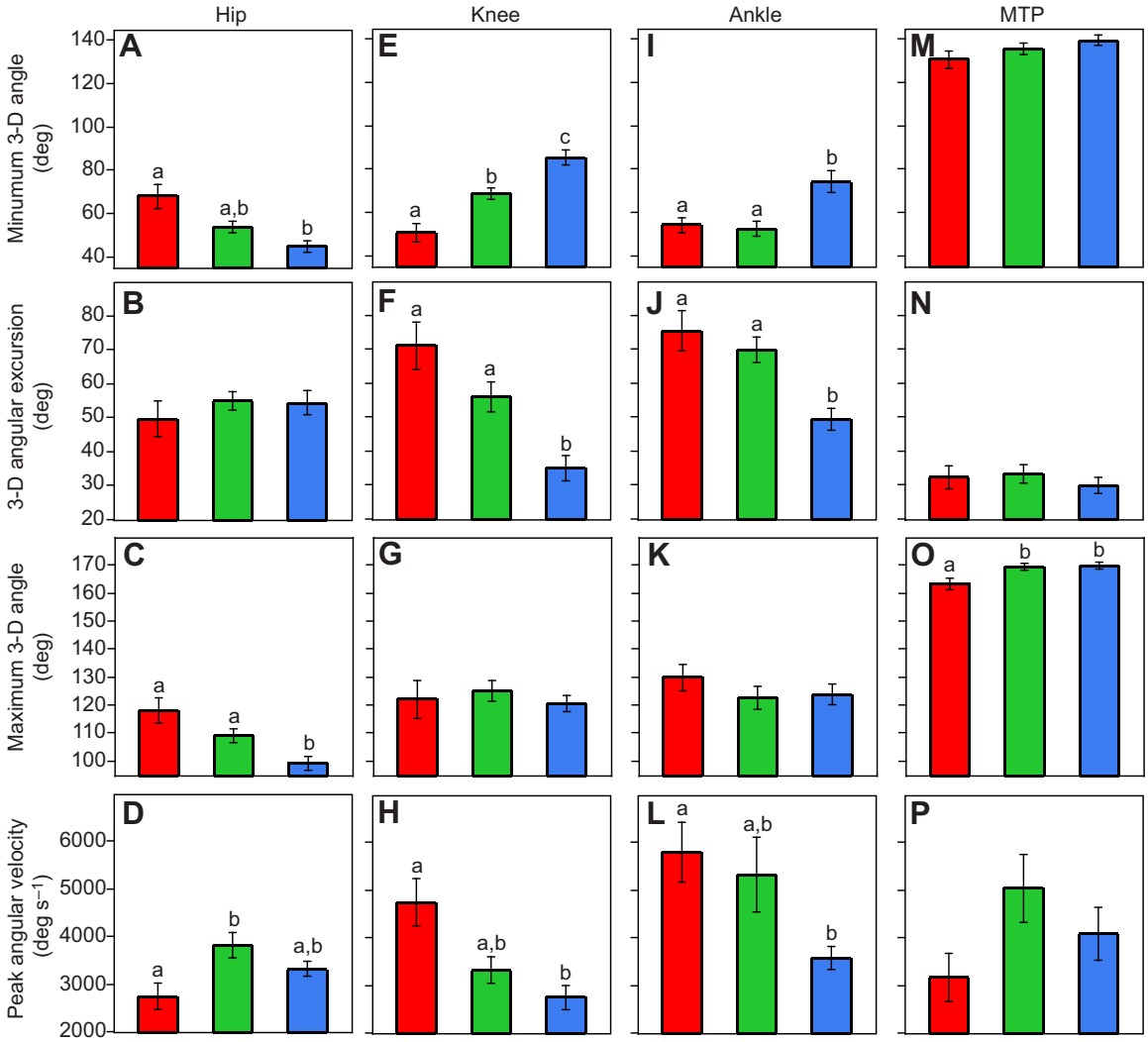

Fig. 5. Per-stride values (means ± s.e.m.) for (A–D) hip, (E–H) knee, (I–L) ankle and (M–P) metatarsophalangeal (MTP) joint three-dimensional (3-D) angles. Colors: red, stride 1; green, stride 2; blue, stride 3. Different letters within a panel denote significantly different groupings (Tukey's HSD *post hoc* tests).

P<0.001; Fig. 3). The univariate mixed models showed that the hip had smaller minimum ($F_{2,18}$=7.95, P=0.003) and maximum 3-D angles ($F_{2,18}$=7.79, P=0.004) as stride number increased (Fig. 5). This resulted in a similar 3-D angular excursion at the hip across all strides ($F_{2,18}$=0.40, P=0.675). Peak 3-D hip angular velocities were slowest during stride 1, fastest during stride 2 and intermediate during stride 3 ($F_{2,18}$=3.90, P=0.039). Most of the joint motion at the hip could be attributed to protraction–retraction and rotation as opposed to abduction–adduction (Fig. 4). Total protraction–retraction angular excursions were ~50 deg whereas total abduction–adduction angular excursions were typically <10 deg (Fig. 6). These data show that, across the first three strides, *S. woodi* generally keep their femur highly abducted and nearly parallel to the ground. Femur rotation was quite different when comparing stride 1 with strides 2 and 3 (overall profile comparison, stride×spline interaction: $F_{28,268}$=549.9, P<0.001): rotational excursions were less pronounced for stride 1 (~15 deg) compared with strides 2 (~30 deg) and 3 (~40 deg), with the plane defined by the thigh and shank being oriented caudally throughout stride 1 (~70–90 deg) but rotating from a more vertical orientation (~40 deg) to a caudal orientation (~75 deg) in strides 2 and 3 (Figs 4, 6).

Knee

The GLMM showed that the overall shape of the kinematic profiles was significantly different across strides (stride×spline interaction: $F_{30,269}$=2.98, P<0.001; Fig. 3). The univariate mixed models showed that the knee had significantly larger minimum angles ($F_{2,18}$=19.03, P<0.001) and smaller angular excursions ($F_{2,18}$=13.38, P<0.001) as stride number increased. Maximum knee angle did not vary across strides ($F_{2,18}$=0.42, P=0.664). Thus, the knee was relatively more flexed near touchdown in the first stride, subsequently sweeping through a greater arc (Figs 3, 5). In contrast, by the third stride, the knee was more extended at touchdown, sweeping through a smaller arc. This contrasting pattern of knee angular kinematics in early *vs* later strides occurs with almost invariant maximum knee angles near lift-off. Peak knee angular velocity showed a significant difference across strides ($F_{2,18}$=6.62, P=0.007) towards decreasing peak velocity during later strides.

Ankle

Kinematic changes in the ankle across strides mirrored those in the knee. The GLMM showed that the overall shape of the kinematic profiles was significantly different across strides (stride×spline

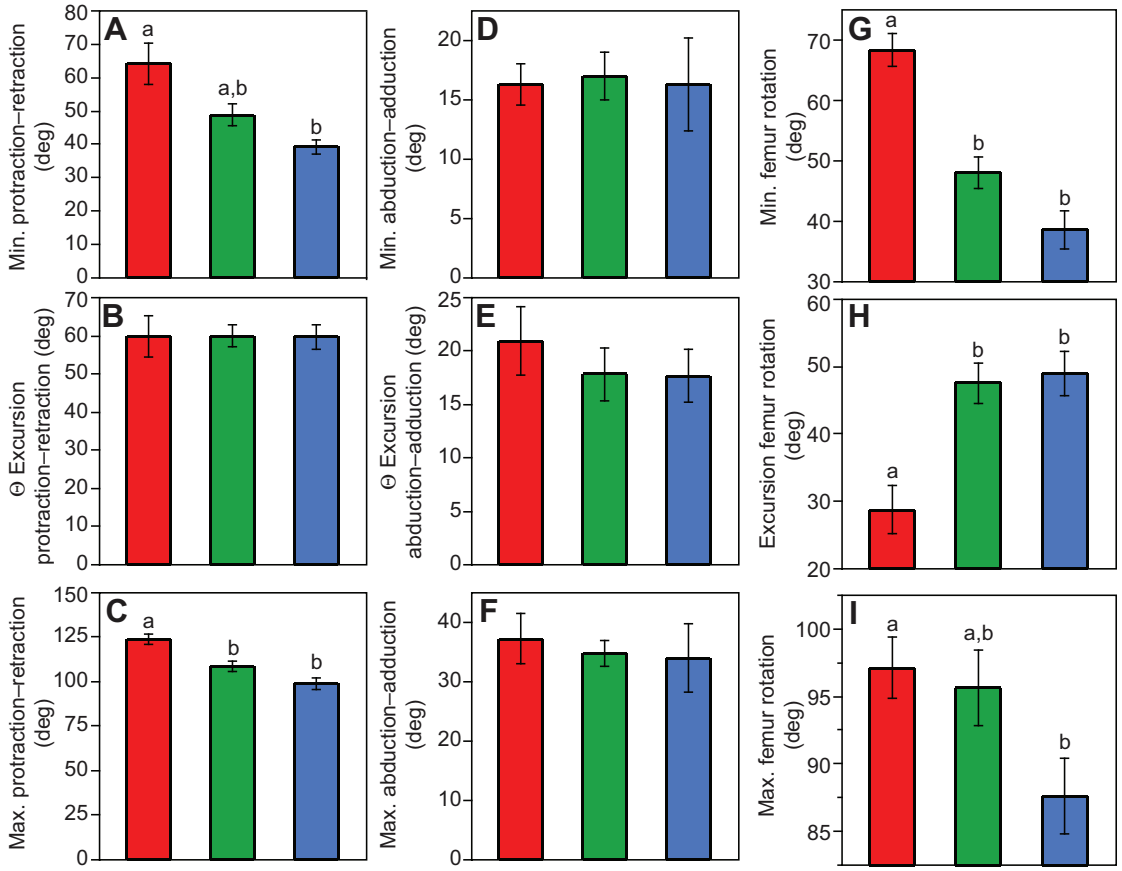

Fig. 6. Per-stride minimum angle, angular excursion and maximum angle values (means ± s.e.m.) for femur (A–C) protraction–retraction, (D–F) abduction–adduction and (G–I) rotation. Colors: red, stride 1; green, stride 2; blue, stride 3. Different letters within a panel denote significantly different groupings (Tukey's HSD *post hoc* tests).

interaction: $F_{30,269}$=1.67, P=0.019; Fig. 3). The univariate mixed models found that minimum joint angle ($F_{2,18}$=7.35, P=0.005) and the total angular excursion ($F_{2,18}$=12.18, P<0.001) varied significantly with stride number. During early strides, the ankle was more flexed near touchdown, subsequently sweeping through a larger arc (Figs 3, 5). In contrast, later strides showed a more extended ankle near touchdown, sweeping through a smaller arc. Like the knee, the variability in angular kinematics in early *vs* late strides occurs with almost invariant maximum ankle angles ($F_{2,18}$=0.73, P=0.495). Peak ankle angular velocity showed a significant difference across strides toward slower speeds with increasing stride number ($F_{2,18}$=7.12, P=0.005).

MTP

The GLMM showed that the overall shape of the kinematic profiles was similar across strides (stride×spline interaction: $F_{30,269}$=0.89, P=0.63; Fig. 3). This concurred with results of the univariate mixed models: minimum joint angle ($F_{2,18}$=1.86, P=0.184), angular excursion ($F_{2,18}$=0.47, P=0.631) and maximum joint angular velocity ($F_{2,18}$=2.35, P=0.124) did not significantly differ with stride number. However, maximum MTP joint angle (i.e. extension) was significantly different across strides ($F_{2,18}$=4.37, P=0.028), with stride 1 having a slightly smaller maximum angle compared with strides 2 and 3 (Fig. 5).

Relationship between joint angular kinematics and whole-animal performance

Maximum trial speed was variable (mean: 1.37 m s^{-1}; range: 0.76–1.95 m s^{-1}), with the high end of the range approaching *S. woodi*'s maximum running speed (Miles, 1994; McElroy and McBrayer, 2010; Higham et al., 2011). Whole-animal acceleration decreased with increasing stride number whereas whole-animal

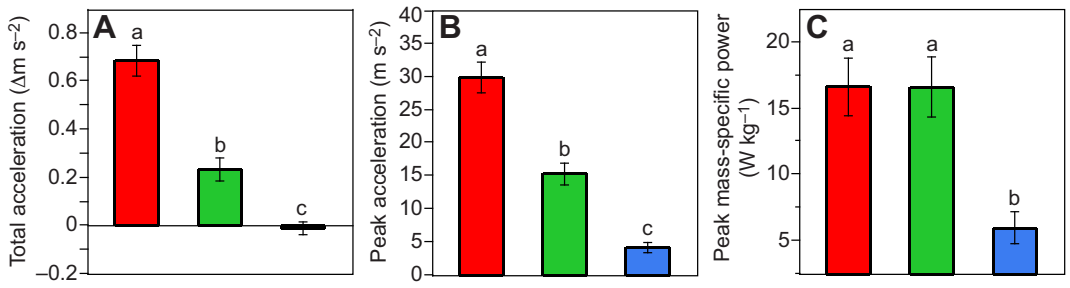

Fig. 7. Per-stride values (means ± s.e.m.) for performance variables. Colors: red, stride 1; green, stride 2; blue, stride 3. Different letters within a panel denote significantly different groupings (Tukey's HSD *post hoc* tests).

mass-specific power was large on stride 1 and 2 but smaller on stride 3 (Fig. 7). In general, the Pearson correlations between per-stride joint angular kinematics and performance were weak (r<0.40) and not significant (P>0.05, Table 1). However, a few of the kinematic variables were significantly correlated with performance (r>0.43) for some strides. For stride 1, MTP and hip angular kinematics were important predictors of final speed and mass-specific power, respectively. Stride 2 had only two significant correlations, between maximum MTP angle and mass-specific power and between maximum knee angle and total acceleration. Stride 3 had the greatest number of significant correlations, with variables from each joint being correlated with final speed, and minimum ankle angle correlating with mass-specific power.

Strong correlations among kinematic variables were apparent (supplementary material Table S1), which could potentially impact the interpretation of the simple Pearson correlations. Bayesian model averaging revealed a few new kinematic variables as important predictors of performance (Table 1); however, this analysis also concurred, in some cases, with the simple correlations. Hierarchical partitioning clearly showed that kinematic collinearity had a large influence on the simple correlations between kinematics and performance (Table 2). When comparing the results of the hierarchical partitioning analysis with the simple correlations, one must first square the simple correlation to compute the variance it explains (e.g. for minimum MTP angle, r=–0.59 and r^2=0.35), and then examine how r^2 is partitioned into independent (e.g. 0.15) *vs* joint (e.g. 0.20) contributions (Table 2). Examining the breakdown of all significant simple correlations, it becomes apparent that most of these simple correlations are due primarily to joint contributions (i.e. collinearity). Thus, collinear patterns between kinematic variables are more important than simple individual effects in explaining the variance in performance.

Separate MANOVAs found that single-legged push-offs exhibited significantly lower locomotor performance than double-legged push-offs (for final speed, total and peak acceleration, and mass-specific power, Wilks' λ=0.545, $F_{2,17}$=7.08, P=0.006). Joint kinematics did not differ between single- and double-legged push-offs (Wilks' λ=0.865, $F_{4,15}$=0.59, P=0.67).

Separate *vs* combined strides analysis

The DFA using step as a classification variable according to joint kinematics was significant (Wilks' λ=0.116, $F_{48,172}$=2.68, P<0.001). The classification table (supplementary material Table S2) showed that most steps were accurately classified as the correct step (22% misclassification rate) and/or the correct stride (10% misclassification rate; stride is based on our grouping of steps). Supplementary material Fig. S1 shows that step 2 is separated from all other steps, steps 2 and 3 group together and steps 4 and 5 group together.

The DFA using step as a classification variable according to locomotor performance was also significant (Wilks' λ=0.103, $F_{16,159.5}$=11.0, P<0.001). The classification table (supplementary material Table S3) showed that most steps were accurately classified as the correct step (25% misclassification rate) and/or the correct stride (8% misclassification rate; stride is based on our grouping). Supplementary material Figs S2 and S3 show that step 1 is separated from all other steps, steps 4 and 5 group together and are almost distinct from step 2, and step 3 is intermediate to step 2 and the step 4/5 group.

The Pearson correlation matrix for the combined strides data set was different from the separate stride matrices (Table 1). Several variables that were significantly correlated with whole-animal performance in the separate stride analysis were not significant once strides were combined (e.g. minimum hip, knee and ankle angles). In addition, several kinematic variables that were never significantly correlated with performance in the separate stride analysis had significant correlations in the combined stride analysis (e.g. minimum knee angle, knee and ankle angular excursion). Mantel tests comparing the combined stride matrix with each separate stride matrix found very small correlation coefficients that were not

Table 2. Results of the hierarchical partitioning analysis

	Stride 1				Stride 3				Combined			
	Final speed		Peak mass-specific power		Final speed		Final speed		Total acceleration		Peak acceleration	
	I	*J*	*I*	*J*	*I*	*J*	*I*	*J*	*I*	*J*	*I*	*J*
Min. hip Θ	–	–	0.12	0.11	0.06	0.22	–	–	–	–	–	–
Min. knee Θ	–	–	–	–	0.15	0.28	–	–	0.11	0.17	0.10	0.17
Min. ankle Θ	0.06	–0.06	–	–	0.10	0.30	0.10	–0.05	–	–	–	–
Min. MTP Θ	0.15	0.20	–	–	0.05	0.17	0.10	0.09	–	–	–	–
Min. rotation Θ	–	–	–	–	–	–	–	–	0.14	0.22	0.15	0.17
Total Θ swept hip	–	–	–	–	0.09	0.16	–	–	–	–	–	–
Total Θ swept knee	–	–	–	–	–	–	–	–	0.08	0.17	0.07	0.20
Total Θ swept ankle	0.10	–0.04	–	–	–	–	0.04	–0.03	0.11	0.18	0.08	0.18
Total Θ swept MTP	0.14	0.28	–	–	0.08	0.20	0.07	0.11	–	–	–	–
Total Θ swept rotation	–	–	0.14	0.16	–	–	–	–	0.07	0.15	–	–
Θ V_{max} hip	–	–	–	–	–	–	–	–	0.10	0.02	–	–
Θ V_{max} knee	–	–	–	–	–	–	–	–	–	–	0.07	0.15
Θ V_{max} ankle	–	–	–	–	0.16	0.04	–	–	–	–	–	–
Θ V_{max} MTP	0.10	0.24	0.13	0.09	0.04	0.18	–	–	–	–	–	–
Θ V_{max} rotation	0.13	0.17	–	–	0.17	0.36	0.15	0.10	–	–	–	–

Only variables with a significant simple Pearson correlation, or 0.75 posterior probability in Bayesian model averaging, were included in the partitioning analysis. *I* is the variance explained by a predictor variable that is independent of the variance explained by other predictors (i.e. not influenced by collinearity) and is always a positive number or zero. *J* is the variance explained by collinearity between predictors. A positive *J* suggests that collinearity has inflated the simple correlation between the predictor and response, whereas a negative *J* suggests that collinearity has suppressed the simple correlation. The square root of the sum of *I* and *J* for each variable is the absolute value of its simple Pearson correlation.

MTP, metatarsophalangeal; Θ, angle; Θ V_{max}, maximum instantaneous angular velocity.

statistically significant (combined strides *vs*: stride 1, r=0.07, P=0.33; stride 2, r=0.21, P=0.08; stride 3, r=0.07, P=0.33), suggesting that the correlation matrices of separate *vs* combined strides analyses were different.

DISCUSSION

Angular kinematics of burst locomotion *vs* steady speed locomotion

The stance phase joint kinematics of *S. woodi* across the first three strides of burst locomotion exhibited both similarities and differences when compared with other lizard species running at near-maximal steady speeds (Reilly and Delancey, 1997; Irschick and Jayne 1999). Irschick and Jayne (Irschick and Jayne, 1999) showed that the femur is retracted and positively rotated throughout stance; in *S. woodi*, the 3-D motion of the hip joint shows a similar pattern (Fig. 2), as do the femur rotation and two-dimensional protraction–retraction angular data (Fig. 3). However, Irschick and Jayne (Irschick and Jayne, 1999) and Reilly and Delancey (Reilly and Delancey, 1997) also showed that the knee and ankle joints undergo flexion during the first half of stance phase followed by extension during the second half while running. For the first two strides in *S. woodi*, the knee and ankle extend throughout the entire stance phase with almost no flexion. However by stride 3, slight flexion of the knee and ankle is apparent during the first half of stance followed by extension during the second half of stance (Fig. 2). This change in joint kinematics suggests that the mechanical function of the joint, and the muscles that power joint motion, are changing dramatically from strides 1 through 3. Therefore, major differences exist between the 3-D kinematics of burst locomotion and the 3-D kinematics of maximum steady running speeds in lizards.

Studies of acceleration in other vertebrates [e.g. greyhounds (Williams et al., 2009) and tammar wallabies (McGowan et al., 2005)] have shown that the knee and ankle undergo flexion–extension during acceleratory strides, similar to that observed in stride 3 in *S. woodi* and other lizards running at near maximal speeds. We did not observe such knee and ankle kinematics in strides 1 and 2 for *S. woodi*. This difference in joint kinematics may be due to a difference in methodology; these studies did not examine locomotion from a standstill, rather they induced animals to start running at 'various distances' from the video's field of view. Thus, it may be that these studies recorded a later stride (third or beyond) in which there was still an acceleration, but the joint kinematics were more similar to those at maximal running speed. Yet another possible explanation for this difference is posture; *S. woodi* has a sprawling gait whereas the greyhound and wallaby have upright gaits.

The joint kinematics of explosive jumping in frogs (Kargo et al., 2002; Nauwelaerts et al., 2005) and *Galago* (Aerts, 1998) are more similar to the joint kinematics observed during strides 1 and 2 in *S. woodi*, i.e. during jumping, the hip, knee, ankle and MTP undergo a pronounced extension without any flexion, except a slight amount at the MTP (Fig. 3). Jumping kinematics in lizards is poorly studied; *Anolis carolinensis* appears to use a countermovement jump that involves flexion–extension at the knee and ankle (Bels et al., 1992). Thus, although the kinematics of the initial locomotor burst in *S. woodi* are quite similar to the jumps of frogs and *Galago* it is unknown how similar they are to jumps in *S. woodi* or other small quadrupeds.

Overall, the kinematics of burst locomotion in *S. woodi* are different from the kinematics of speed changes (i.e. accelerations) in animals that are already moving [e.g. greyhounds (Williams et al., 2009)] and of other lizards running at maximal speeds (Irschick and Jayne, 1999). This suggests that the kinematics and biomechanics of maximum acceleration and power, which occur during burst locomotion, cannot simply be extrapolated from data collected during running accelerations (Roberts and Scales, 2002; McGowan et al., 2005; Williams et al., 2009). Rather, future studies need to explicitly quantify the events happening during each of the first few strides of burst locomotion in both a comparative context and within a uniform experimental framework.

Kinematic predictors of locomotor performance

Previous studies have found that proximal limb musculature is the most important predictor of acceleration in lizards (Reilly and Delancey, 1997; Nelson and Jayne, 2001; Vanhooydonck et al., 2006a). Our results partially agree with these findings in that femur rotation, minimum hip angle and maximum knee angular velocity were significantly correlated with acceleration or mass-specific power (Table 1). However, there was generally a lack of correlation between kinematics and acceleration or mass-specific power across the first three strides of burst locomotion. This lack of correlation suggests that other variables we did not measure (e.g. ground-reaction forces, joint torques, joint work, joint power and/or muscle forces) may be more important predictors of acceleration or power than angular kinematics.

The distal hindlimb elements (e.g. metatarsus and toes) are the most important predictors of maximum running speed in lizards (Miles, 1994; Bauwens et al., 1995; Irschick and Jayne, 1999; Vanhooydonck et al., 2006a; Miles et al., 2007). We found that MTP (strides 1 and 3) and ankle (stride 3) kinematics were significantly correlated with final sprint speed (Table 1). In stride 1, MTP kinematics clearly impacted the final speed achieved by *S. woodi* at the end of stride 3 (Table 1). Why kinematics during stride 1 should have an impact on the final speed achieved by the animal is unclear. For example, MTP kinematics did not affect acceleration performance during stride 1 and thus greater maximum speeds were not achieved *via* the effect of MTP kinematics on acceleration performance for stride 1. In addition, MTP kinematics were not different for individuals lizards using a double- *vs* single-legged push-off. One possibility is that the correlation between MTP kinematics and final speed found for stride 1 is explained by an effect of stride 1 MTP kinematics on performance in stride 2. In fact, MTP kinematics in stride 1 were significantly correlated with peak acceleration in stride 2 (minimum MTP angle: peak acceleration, r=–0.46; MTP excursion: peak acceleration, r=0.45; MTP angular velocity: peak acceleration, r=0.54; all P<0.05). Several possible mechanisms could explain this finding. In humans, greater joint angular excursion in stride 1 has been suggested to result in the center of mass being positioned further in front of the feet during stride 2, thereby enhancing the effectiveness of stride 2 joint extension on horizontal force production and acceleration (Harland and Steele, 1997; Bezodis et al., 2008). In a quadruped, this could manifest as the center of mass being positioned further in front of the hindfoot prior to touchdown, such that upon touchdown the hindlimb portion of the ground-reaction force vector is orientated more horizontally. Another possibility is that larger MTP angular excursion in stride 1 could pre-position the distal limb musculature for the next stance phase such that it contracts over a more optimal portion of its length–tension curve (Gordon et al., 1966). Future studies that integrate measurement of ground-reaction forces, whole-body dynamics and *in vivo* muscle activity as well as quantification of *in vitro* muscle physiology for these muscles would be useful for discovering the causal mechanism underlying the correlation between MTP kinematics and whole-animal performance.

Stride 3 had several significant correlations between kinematics and final speed. These correlations imply that greater final sprinting speeds are obtained with: (1) more extended hip, knee and ankle at touchdown (i.e. greater minimum angle), (2) greater MTP joint excursion and speed, (3) smaller hip joint excursion and (4) greater ankle extension at toe-off (Table 1). Coupled with the correlations found for stride 1, it appears that in *S. woodi*, the kinematics of the ankle and MTP joints are the key determinants of final sprinting speed. The fiber-type composition of the gastrocnemius muscle (an ankle extensor) in *S. woodi* was recently shown to be correlated with both maximum sprinting speed and acceleration capacity (Higham et al., 2011). In addition, functional studies of *Sceloporus clarki* suggest that plantar flexion is an important component of thrust generation during sub-maximal steady speed running (e.g. Reilly and Delancey, 1997). Finally, several studies of phrynosomatine lizards have shown a correlation between distal limb morphology, particularly metatarsus length, and maximum sprinting performance (e.g. Miles, 1994; Irschick and Jayne, 1999). Thus among phrynosomatine lizards, it appears that the distal bony elements and musculature of the hindlimb are the key determinants of maximum locomotor performance. However, additional data are needed on the physiological properties of limb muscles (e.g. ambiens, flexor digitorum communis). Finally, when linking joint motion and locomotor performance, one must be cautious: only a computational musculoskeletal model coupled with inverse dynamic analysis will definitively quantify joint moments. Only with such data in hand may we fully assess the differential contribution of each joint and its musculature to locomotion performance (e.g. Aerts, 1998).

Although the distal limb appears to be the most important predictor of burst performance in *S. woodi* and perhaps the Phrynosomatidae, this may not hold true for other groups. For example, Vanhooydonck et al. (Vanhooydonck et al., 2006a) showed that the mass of the knee extensors was the most important muscular predictor of acceleration capacity and maximum speed for a sample of 16 *Anolis* species. In addition, Curtin et al. (Curtin et al., 2005) showed that the power output of the entire mass of the retractors and extensors of the hindlimb are required to power maximal accelerations in *Acanthodactylus*, suggesting that function at all joints is important for achieving maximum acceleration and speed. Finally, in mammals, the pattern is complex and species specific; greyhounds rely on hip retractors and ankle extensors (Williams et al., 2009), wallabies rely on ankle extensors coupled with power transfer from the proximal limb muscles (McGowan et al., 2005), and humans rely on the femur retractors and knee extensors (Delecluse, 1997). What is emerging from the study of the functional basis of acceleration across taxa is that evolution generates many different functional solutions (i.e. many-to-one mapping) to achieve greater acceleration capacity (Alfaro et al., 2004; Bock, 1959; Wainwright, 2007). Although the discovery of broad general principles is a central goal in science, the emerging relationships between morphology, function and acceleration performance indicates that different clades find different functional solutions to increase performance (Vanhooydonck et al., 2006a), and that maximizing acceleration capacity may be better defined by divergent functional mechanisms than by any general principle.

Separate *vs* combined strides analysis

An important finding from our study is that the correlation structure between joint angular kinematics and performance changes based on how one analyzes a burst locomotor event. When all strides were combined, most of the significant correlations between speed or mass-specific power and joint kinematics disappeared and several new correlations between acceleration and kinematics appeared (Table 1). Thus, had we pooled kinematic data across strides, our interpretations of the functional basis of performance would have been drastically altered (e.g. knee kinematics seem to be important predictors of acceleration in the combined analysis). In our opinion, separate stride analysis is the best method and this seems justified for several reasons. First, we clearly show that limb joint kinematics and locomotor performance are different from strides 1 through 3 during the burst locomotor event (e.g. Figs 2–7). Thus, by combining the kinematic data, one is ignoring a potentially important source of variation (i.e. stride to stride) that could potentially mask or even reverse our interpretation of function (i.e. knee *vs* ankle or MTP kinematic correlations; Table 1). This issue is even further amplified because of the collinear nature of limb kinematics (supplementary material Table S1) and the correlation between limb kinematics and performance, as shown by the hierarchical partitioning analysis (Table 2). Second, from the perspective of the organism, burst locomotion is a very different behavior than speed changes (i.e. acceleration) while running. The animal starts at a complete standstill and then suddenly engages in rhythmic cycling of the limbs, whereas, for an animal already in motion, it simply has to alter the cyclical pattern of muscle activation and joint kinematics. Both behaviors involve acceleration, even large accelerations, but they seem to be fundamentally different in kinematics and function. The fact that most previous studies have used a ‘combined’ strides approach likely stems from the history of how we have studied steady-speed locomotion. Most studies of steady-speed locomotion essentially ignore ‘stride number’ because once the animal is moving at steady speed, stride-to-stride variation in kinematics and mechanics are minimal. This is why using a treadmill for steady-speed studies works well. It should be noted that even the present study has a shortfall: we combined steps into strides, which was justified based on methodological constraints and statistical grounds (supplementary material Figs S1–S3, Tables S2, S3). Although this seems acceptable for the study of burst locomotor in *S. woodi*, it may not be in other organisms. Based on these findings, we feel that it is important to find common methodologies by which we can expand our functional understanding of burst locomotion, acceleration performance and acceleration biomechanics.

ACKNOWLEDGEMENTS

We thank Anna Baur, Shea Diaz, Melissa Strickland and Allyson Wilson for assistance running lizards, trimming videos for analysis and animal care. We thank Allan Strand and Ralph Mac Nally for advice regarding Bayesian model averaging and hierarchical partitioning.

FUNDING

This work was supported by start-up funds provided by the College of Charleston to E.J.M.

REFERENCES

Aerts, P. (1998). Vertical jumping in *Galago senegalensis*: the quest for a hidden power amplifier. *Philos. Trans. R. Soc. Lond. B* **353**, 1607-1620.

Alfaro, M. E., Bolnick, D. I. and Wainwright, P. C. (2004). Evolutionary dynamics of complex biomechanical systems: an example using the four-bar mechanism. *Evolution* **85**, 495-503.

Arnold, S. J. (1983). Morphology, performance and fitness. *Am. Zool.* **23**, 347-361.

Bauwens, D., Garland, T., Jr, Castilla, A. M. and Van Damme, R. (1995). Evolution of sprint speed in lacertid lizards: morphological, physiological, and behavioral covariation. *Evolution* **49**, 848-863.

Bels, V. L. and Theys, J.-P., Bennett, M. R. and Legrand, L. (1992). Biomechanical analysis of jumping in *Anolis carolinensis* (Reptilia: Iguanidae). *Copeia* **1992**, 492-504.

Bezodis, N. E., Trewartha, G. and Salo, A. I. (2008). Understanding elite sprint starting performance through an analysis of joint kinematics. In *Proceedings of the XXVI International Conference on Biomechanics in Sports* (ed. Y.-H. Kwon, J. Shim, J. K. Shim and I. S. Shin), pp. 498-501. Seoul, Korea: Rainbow Books.

Bock, W. J. (1959). Preadaptation and multiple evolutionary pathways. *Evolution* **13**, 194-211.
Calsbeek, R. and Irschick, D. J. (2007). The quick and the dead: locomotor performance and natural selection in island lizards. *Evolution* **61**, 2493-2503.
Chevan, A. and Sutherland, M. (1991). Hierarchical partitioning. *Am. Stat.* **45**, 90-96.
Clemente, C. J., Withers, P. C., Thompson, G. and Lloyd, D. (2008). Why go bipedal? Locomotion and morphology in Australian agamid lizards. *J. Exp. Biol.* **211**, 2058-2065.
Cullum, A. J. (1999). Didge - Image Digitizing Software. Version 2.0.
Curtin, N., Woledge, R. and Aerts, P. (2005). Muscle directly meets the vast power demands in agile lizards. *Proc. R. Soc. Lond. B* **272**, 581-584.
Delecluse, C. (1997). Influence of strength training on sprint running performance: current findings and implications for training. *Sports Med.* **24**, 147-156.
Ellison, A. M. (1996). An introduction to Bayesian inference for ecological research and environmental decision-making. *Ecol. Appl.* **6**, 1036-1046.
Garland, T., Jr and Losos, J. B. (1994). Ecological morphology of locomotor performance in squamate reptiles. In *Ecological Morphology: Integrative Organismal Biology* (ed. P. C. Wainwright and S. M. Reilly), pp. 240-302. Chicago, IL: University of Chicago Press.
Gordon, A. M., Huxley, A. F. and Julian, F. J. (1966). The variation in isometric tension with sarcomere length in vertebrate muscle fibers. *J. Physiol.* **184**, 170-192.
Harland, M. J. and Steele, J. R. (1997). Biomechanics of the sprint start. *Sports Med.* **23**, 11-20.
Hedrick, T. L. (2008). Software techniques for two- and three-dimensional kinematic measurements of biological and biomimetic systems. *Bioinspir. Biomim.* **3**, 034001.
Higham, T. E., Korchari, P. G. and McBrayer, L. D. (2011). How muscles define maximum running performance in lizards: an analysis using swing and stance phase muscles. *J. Exp. Biol.* **214**, 1685-1691.
Husak, J. F., Lovern, M. B., Fox, S. F. and Van Den Bussche, R. A. (2006). Faster lizards sire more offspring: sexual selection on whole-animal performance. *Evolution* **60**, 2122-2130.
Irschick, D. J. and Garland, T., Jr (2001). Integrating function and ecology in studies of adaptation: investigations of locomotor capacity as a model system. *Ann. Rev. Ecol. Syst.* **32**, 367-396.
Irschick, D. J. and Jayne, B. C. (1999). Comparative three-dimensional kinematics of the hindlimb for high-speed bipedal and quadrupedal locomotion of lizards. *J. Exp. Biol.* **202**, 1047-1065.
Irschick, D. J. and Losos, J. B. (1998). A comparative analysis of the ecological significance of locomotor performance in Caribbean *Anolis* lizards. *Evolution* **52**, 219-226.
Jayne, B. C. and Irschick, D. J. (1999). Effects of incline and speed on the three-dimensional hindlimb kinematics of a generalized iguanian lizard (Dipsosaurus dorsalis). *J. Exp. Biol.* **202**, 143-159.
Kargo, W. J., Nelson, F. and Rome, L. C. (2002). Jumping in frogs: assessing the design of the skeletal system by anatomically realistic modeling and forward dynamic simulation. *J. Exp. Biol.* **205**, 1683-1702.
Kass, R. E. and Raftery, A. E. (1995). Bayes factors. *J. Am. Stat. Assoc.* **90**, 773-795.
Kramer, D. L. and McLaughlin, R. L. (2001). The behavioural ecology of intermittent locomotion. *Am. Zool.* **41**, 137-153.
Le Galliard, J.-F., Clobert, J. and Ferriere, R. (2004). Physical performance and Darwinian fitness in lizards. *Nature* **432**, 502-505.
Losos, J. B. (1990). Ecomorphology, performance capability, and scaling of West Indian *Anolis* lizards: an evolutionary analysis. *Ecol. Monogr.* **60**, 369-388.
Mac Nally, R. (2000). Regression and model-building in conservation biology, biogeography and ecology: the distinction between and reconciliation of predictive and 'explanatory' models. *Biodivers. Conserv.* **9**, 655-671.
Mac Nally, R. (2002). Multiple regression and inference in ecology and conservation biology: further comments on identifying important predictor variables. *Biodivers. Conserv.* **11**, 1397-1401.
McElroy, E. J. and McBrayer, L. D. (2010). Getting up to speed: acceleration strategies in the Florida scrub lizard, *Sceloporus woodi*. *Physiol. Biochem. Zool.* **83**, 643-653.
McElroy, E. J., Meyers, J. J., Reilly, S. M. and Irschick, D. J. (2007). Dissecting the roles of behaviour and habitat on the locomotion of a lizard, *Urosaurus ornatus*. *Anim. Behav.* **73**, 359-365.
McElroy, E. J., Hickey, K. H. and Reilly, S. M. (2008). The correlated evolution of biomechanics, gait, and foraging mode in lizards. *J. Exp. Biol.* **211**, 1029-1040.
McGowan, C. P., Baudinette, R. V. and Biewener, A. A. (2005). Joint work and power associated with acceleration and deceleration in tammar wallabies (*Macropus eugenii*). *J. Exp. Biol.* **208**, 41-53.
Miles, D. B. (1994). Covariation between morphology and locomotory performance in sceloporine lizards. In *Lizard Ecology: Historical and Experimental Perspectives* (ed. L. J. Vitt and E. R. Pianka), pp. 207-236. Princeton, NJ: Princeton University Press.
Miles, D. B., Losos, J. B. and Irschick, D. J. (2007). Morphology, performance, and foraging mode. In *Lizard Ecology*: *The Evolutionary Consequences of Foraging Mode* (ed. S. M. Reilly, L. B. McBrayer and D. B. Miles), pp. 49-93. Cambridge: Cambridge University Press.
Nauwelaerts, S. and Aerts, P. (2003). Propulsive impulse as a covarying performance measure in the comparison of the kinematics of swimming and jumping in frogs. *J. Exp. Biol.* **206**, 4341-4351.
Nauwelaerts, S., Stamhuis, E. and Aerts, P. (2005). Swimming and jumping in a semi-aquatic frog. *Anim. Biol.* **55**, 3-15.
Nelson, F. E. and Jayne, B. C. (2001). The effects of speed on the *in vivo* activity and length of a limb muscle during the locomotion of an iguanian lizard, *Dipsosaurus dorsalis*. *J. Exp. Biol.* **204**, 3507-3522.
Quinn, G. P. and Keough, M. J. (2003). *Experimental Design and Data Analysis for Biologists.* Cambridge: Cambridge University Press.
R Development Core Team (2009). R: A language and environment for statistical computing. Vienna, Austria: R Foundation for Statistical Computing, http://www.R-project.org.
Raftery, A. E., Hoeting, J. A. and Volinsky, C. T. (2005). BMA: Bayesian model averaging. R package version 2.3. http://CRAN.R-project.org/package=BMA
Reilly, S. M. and DeLancey, M. L. (1997). Sprawling locomotion in the lizard *Sceloporus clarkii*: the effects of speed on gait, hindlimb kinematics, and axial bending during walking. *J. Zool. Lond.* **243**, 417-433.
Reilly, S. M. and Wainwright, P. C. (1994). Conclusion: ecological morphology and the power of integration. In *Ecological Morphology: Integrative Organsimal Biology* (ed. P. C. Wainwright and S. M. Reilly), pp. 339-354. Chicago, IL: University of Chicago Press.
Roberts, T. J. and Scales, J. A. (2002). Mechanical power output during running accelerations in wild turkeys. *J. Exp. Biol.* **205**, 1485-1494.
Vanhooydonck, B., Herrel, A. and Irschick, D. J. (2006a). The quick and the fast: the evolution of acceleration capacity in *Anolis* lizards. *Evolution* **60**, 2137-2147.
Vanhooydonck, B., Herrel, A. and Irschick, D. J. (2006b). Out on a limb: the differential effect of substrate diameter on acceleration capacity in *Anolis* lizards. *J. Exp. Biol.* **209**, 4515-4523.
Wainwright, P. C. (2007). Functional versus morphological diversity in macroevolution. *Annu. Rev. Ecol. Evol. Syst.* **38**, 381-401.
Walsh, C. and Mac Nally, R. (2008). hier.part: hierarchical partitioning. R package version 1.0-3. http://CRAN.R-project.org/package=hier.part
Williams, S. B., Usherwood, J. R., Jespers, K., Channon, A. J. and Wilson, A. M. (2009). Exploring the mechanical basis for acceleration: pelvic limb locomotor function during accelerations in racing greyhounds (*Canis familiaris*). *J. Exp. Biol.* **212**, 50-65.
Woltring, H. J. (1986). A Fortran package for generalized, cross-validatory spline smoothing and differentiation. *Adv. Eng. Softw.* **8**, 104-113.

Table S1. Pearson product-moment correlation matrices between kinematic variables

	Min Hip Θ	Min Knee Θ	Min Ankle Θ	Min MTP Θ	Min Rot. Θ	Θ –Swept Hip	Θ –Swept Knee	Θ –Swept Ankle	Θ –Swept MTP	Θ –Swept Rot.	Max Hip Θ	Max Knee Θ	Max Ankle Θ	Max MTP Θ	Max Rot. Θ	Θ V-Max Hip	Θ V-Max Knee	Θ V-Max Ankle	Θ V-Max MTP	Θ V-Max Rot.
Stride 1																				
Min Hip Θ	1.00																			
Min Knee Θ	0.73	1.00																		
Min Ankle Θ	0.21	0.03	1.00																	
Min MTP Θ	0.21	0.21	0.05	1.00																
Min Rotation Θ	0.84	0.79	0.06	0.40	1.00															
Θ –Swept Hip	-0.67	-0.37	-0.35	-0.04	-0.51	1.00														
Θ –Swept Knee	-0.50	-0.36	-0.29	0.16	-0.41	0.89	1.00													
Θ –Swept Ankle	-0.07	0.18	-0.58	0.18	0.11	0.63	0.72	1.00												
Θ –Swept MTP	-0.21	-0.05	-0.13	-0.87	-0.36	0.27	0.09	0.05	1.00											
Θ –Swept Rotation	-0.68	-0.53	-0.07	-0.50	-0.78	0.42	0.22	-0.20	0.57	1.00										
Max Hip Θ	0.49	0.49	-0.14	0.22	0.47	0.32	0.40	0.65	0.05	-0.38	1.00									
Max Knee Θ	-0.04	0.29	-0.28	0.30	0.10	0.67	0.79	0.85	0.06	-0.12	0.74	1.00								
Max Ankle Θ	0.07	0.23	0.02	0.26	0.18	0.51	0.67	0.80	-0.03	-0.29	0.69	0.84	1.00							
Max MTP Θ	0.06	0.35	-0.12	0.54	0.19	0.39	0.48	0.46	-0.05	-0.04	0.53	0.72	0.48	1.00						
Max Rotation Θ	-0.07	0.11	-0.03	-0.32	-0.03	0.04	-0.14	-0.18	0.48	0.65	-0.03	-0.07	-0.24	0.17	1.00					
Θ V-Max Hip	-0.27	-0.28	0.07	-0.30	-0.29	0.34	0.28	-0.06	0.43	0.55	0.06	0.10	-0.02	0.14	0.54	1.00				
Θ V-Max Knee	-0.13	-0.18	0.13	-0.06	-0.18	0.39	0.57	0.26	0.25	0.27	0.29	0.46	0.41	0.31	0.20	0.79	1.00			
Θ V-Max Ankle	0.12	0.11	-0.06	-0.20	0.13	0.16	0.28	0.31	0.32	0.14	0.34	0.36	0.33	0.14	0.39	0.60	0.75	1.00		
Θ V-Max MTP	-0.19	-0.01	-0.09	-0.69	-0.29	0.15	0.09	0.06	0.74	0.53	-0.07	0.09	0.01	-0.13	0.50	0.54	0.45	0.57	1.00	
Θ V-Max Rotation	-0.10	-0.01	-0.25	-0.36	-0.08	0.19	0.15	0.18	0.51	0.42	0.09	0.15	0.04	0.15	0.57	0.38	0.26	0.51	0.54	1.00
Stride 2																				
Min Hip Θ	1.00																			
Min Knee Θ	-0.03	1.00																		
Min Ankle Θ	-0.38	0.47	1.00																	
Min MTP Θ	-0.20	-0.11	0.24	1.00																
Min Rotation Θ	0.47	-0.55	-0.52	-0.03	1.00															
Θ –Swept Hip	-0.64	-0.25	-0.11	-0.07	0.00	1.00														
Θ –Swept Knee	0.25	-0.59	-0.20	0.35	0.58	0.22	1.00													
Θ –Swept Ankle	0.23	-0.33	-0.33	0.08	0.46	0.35	0.82	1.00												
Θ –Swept MTP	-0.11	0.14	-0.17	-0.87	-0.22	0.28	-0.31	-0.03	1.00											
Θ –Swept Rotation	-0.10	0.43	0.04	-0.57	-0.50	0.36	-0.41	-0.01	0.59	1.00										
Max Hip Θ	0.57	-0.32	-0.53	-0.29	0.52	0.41	0.51	0.61	0.17	0.26	1.00									
Max Knee Θ	0.29	0.07	0.13	0.34	0.27	0.08	0.77	0.75	-0.27	-0.16	0.37	1.00								
Max Ankle Θ	-0.11	0.09	0.53	0.27	-0.02	0.22	0.57	0.62	-0.17	0.03	0.11	0.78	1.00							
Max MTP Θ	-0.60	0.06	0.14	0.20	-0.48	0.42	0.06	0.08	0.31	0.09	-0.23	0.12	0.19	1.00						
Max Rotation Θ	0.34	-0.05	-0.43	-0.62	0.39	0.38	0.10	0.41	0.43	0.61	0.75	0.08	0.01	-0.34	1.00					
Θ V-Max Hip	0.07	-0.23	-0.13	0.11	0.40	0.42	0.40	0.34	-0.12	0.06	0.49	0.31	0.20	-0.03	0.43	1.00				
Θ V-Max Knee	0.25	-0.28	-0.06	0.20	0.53	0.25	0.81	0.78	-0.26	-0.19	0.52	0.78	0.66	-0.15	0.28	0.34	1.00			
Θ V-Max Ankle	0.27	-0.43	-0.44	0.06	0.59	0.35	0.76	0.87	-0.12	-0.03	0.62	0.60	0.42	-0.12	0.51	0.50	0.79	1.00		
Θ V-Max MTP	0.10	0.20	-0.28	-0.43	0.01	-0.03	-0.17	0.11	0.43	0.29	0.03	-0.06	-0.13	0.03	0.31	0.01	-0.10	0.23	1.00	
Θ V-Max Rotation	0.25	0.47	0.05	-0.45	-0.23	-0.02	-0.30	-0.01	0.34	0.71	0.27	0.00	0.03	-0.19	0.55	0.11	-0.09	-0.04	0.06	1.00
Stride 3																				
Min Hip Θ	1.00																			
Min Knee Θ	0.58	1.00																		
Min Ankle Θ	0.56	0.67	1.00																	
Min MTP Θ	-0.21	-0.09	0.07	1.00																

Min Rotation Θ	-0.42	-0.44	-0.61	0.26	1.00															
Θ –Swept Hip	-0.75	-0.66	-0.60	-0.10	0.50	1.00														
Θ –Swept Knee	-0.50	-0.67	-0.40	0.12	0.28	0.72	1.00													
Θ –Swept Ankle	-0.43	-0.48	-0.69	-0.33	0.24	0.51	0.58	1.00												
Θ –Swept MTP	0.27	0.18	-0.01	-0.85	-0.08	0.04	-0.20	0.14	1.00											
Θ –Swept Rotation	0.06	0.12	0.04	-0.73	-0.60	0.05	0.09	0.47	0.42	1.00										
Max Hip Θ	-0.11	-0.42	-0.45	-0.39	0.31	0.73	0.58	0.43	0.35	0.17	1.00									
Max Knee Θ	0.07	0.36	0.30	0.04	-0.17	0.12	0.45	0.15	-0.04	0.26	0.23	1.00								
Max Ankle Θ	0.34	0.48	0.74	-0.21	-0.63	-0.36	-0.02	-0.03	0.11	0.50	-0.22	0.55	1.00							
Max MTP Θ	0.11	0.16	0.11	0.29	0.32	-0.12	-0.15	-0.34	0.26	-0.56	-0.07	0.00	-0.17	1.00						
Max Rotation Θ	-0.46	-0.34	-0.62	-0.57	0.39	0.59	0.42	0.80	0.40	0.50	0.53	0.12	-0.11	-0.30	1.00					
Θ V-Max Hip	-0.12	-0.09	-0.38	-0.15	0.37	0.37	0.16	0.35	0.24	-0.09	0.44	0.09	-0.20	0.16	0.29	1.00				
Θ V-Max Knee	0.12	-0.05	-0.11	-0.34	-0.11	0.10	0.44	0.60	0.20	0.50	0.30	0.49	0.41	-0.27	0.46	0.32	1.00			
Θ V-Max Ankle	-0.03	-0.23	-0.18	-0.52	0.06	0.29	0.39	0.56	0.45	0.49	0.46	0.22	0.26	-0.14	0.63	0.31	0.68	1.00		
Θ V-Max MTP	0.28	0.38	0.34	-0.39	-0.23	-0.01	-0.29	-0.28	0.43	0.24	0.23	0.10	0.21	0.06	0.03	0.15	-0.04	0.28	1.00	
Θ V-Max Rotation	0.35	0.37	0.34	-0.55	-0.65	-0.29	-0.19	0.07	0.48	0.73	-0.05	0.21	0.53	-0.14	0.14	-0.05	0.44	0.42	0.44	1.00
Combined																				
Min Hip Θ	1.00																			
Min Knee Θ	0.02	1.00																		
Min Ankle Θ	-0.10	0.52	1.00																	
Min MTP Θ	-0.09	0.22	0.18	1.00																
Min Rotation Θ	0.59	-0.45	-0.48	-0.02	1.00															
Θ –Swept Hip	-0.64	-0.25	-0.31	-0.03	-0.13	1.00														
Θ –Swept Knee	0.01	-0.66	-0.44	0.02	0.40	0.54	1.00													
Θ –Swept Ankle	0.20	-0.38	-0.62	-0.07	0.45	0.43	0.79	1.00												
Θ –Swept MTP	-0.05	0.00	-0.13	-0.84	-0.12	0.21	-0.02	0.09	1.00											
Θ –Swept Rotation	-0.51	0.26	0.13	-0.33	-0.75	0.31	-0.23	-0.18	0.43	1.00										
Max Hip Θ	0.55	-0.24	-0.43	-0.13	0.58	0.33	0.59	0.68	0.16	-0.29	1.00									
Max Knee Θ	0.04	0.17	-0.04	0.25	0.06	0.45	0.63	0.64	-0.03	-0.03	0.53	1.00								
Max Ankle Θ	0.13	0.10	0.33	0.11	0.02	0.18	0.47	0.53	-0.04	-0.07	0.36	0.73	1.00							
Max MTP Θ	-0.24	0.40	0.11	0.45	-0.24	0.29	0.00	0.02	0.10	0.10	0.03	0.42	0.15	1.00						
Max Rotation Θ	0.14	-0.27	-0.50	-0.50	0.38	0.25	0.25	0.39	0.43	0.33	0.42	0.04	-0.07	-0.20	1.00					
Θ V-Max Hip	-0.24	-0.01	-0.10	-0.07	-0.12	0.37	0.13	0.06	0.20	0.36	0.10	0.16	-0.04	0.21	0.33	1.00				
Θ V-Max Knee	0.22	-0.42	-0.15	-0.17	0.35	0.21	0.69	0.53	0.12	-0.10	0.48	0.47	0.48	-0.11	0.36	0.33	1.00			
Θ V-Max Ankle	0.27	-0.31	-0.34	-0.20	0.40	0.17	0.54	0.59	0.16	-0.05	0.50	0.39	0.35	-0.10	0.51	0.41	0.72	1.00		
Θ V-Max MTP	-0.09	0.22	0.00	-0.41	-0.24	0.08	-0.13	-0.03	0.51	0.40	-0.03	0.05	-0.04	0.08	0.22	0.30	0.03	0.27	1.00	
Θ V-Max Rotation	0.00	0.16	0.02	-0.38	-0.22	0.06	-0.02	0.09	0.45	0.48	0.06	0.14	0.13	0.05	0.36	0.23	0.18	0.26	0.34	1.00

Table S2. Classification table for discriminant function analysis (DFA) using step as a classification variable and kinematic variables as covariates

	Step no. as classified by DFA						
Actual step no.	1	2	3	4	5	Misclassified steps (%)	Misclassified strides (%)
1	18	*1*	*1*	0	0	10	10
2	0	3	2	*1*	0	50	17
3	*1*	3	9	0	*1*	36	14
4	0	0	0	6	0	0	0
5	0	0	*1*	2	11	21	7

Misclassified steps is the total percentage of steps not classified as the correct step (the overall misclassification rate was 22%). Misclassified strides is the total percentage not classified correctly using our stride based grouping (step 1=stride 1; steps 2 and 3=stride 2; steps 4 and 5=stride 3). Numbers in italics represent data points that would still be misclassified using our stride-based grouping (six out of 60).

Table S3. Classification table for discriminant function analysis (DFA) using step as a classification variable and performance variables as covariates

	Step no. as classified by DFA						
Actual step no.	1	2	3	4	5	Misclassified steps (%)	Misclassified strides (%)
1	17	*2*	*1*	0	0	15	15
2	0	5	0	*1*	0	17	17
3	0	3	9	*2*	0	36	14
4	0	0	0	5	1	17	0
5	0	0	*1*	4	9	36	7

Misclassified steps is the total percentage of steps not classified as the correct step (the overall misclassification rate was 25%). Misclassified strides is the total percentage not classified correctly using our stride based grouping (step 1=stride 1; steps 2 and 3=stride 2; steps 4 and 5=stride 3). Numbers in italics represent data points that would still be misclassified using our stride-based grouping (seven out of 60).